J Solid State Electrochem (2001) 5: 50–56

ORIGINAL PAPER

M. Mohan Rao · M. Jayalakshmi · O. Schäf
H. Wulff · U. Guth · F. Scholz

Electrochemical behaviour of solid lithium cobaltate ($LiCoO_2$) and lithium manganate ($LiMn_2O_4$) in an aqueous electrolyte system

Received: 30 August 1999 / Accepted: 11 November 1999

Abstract Lithium cobaltate ($LiCoO_2$) and lithium manganate ($LiMn_2O_4$) were synthesized by self-propagating high-temperature combustion and their phase purity and composition were characterized by X-ray diffraction and inductively coupled plasma spectroscopy. These transition metal oxides were mechanically immobilized on the surface of paraffin-impregnated graphite electrodes and their cyclic voltammetric behaviour in aqueous alkali electrolytes was examined. It was shown that both the oxides undergo proton insertion upon the reduction of Co^{3+} to Co^{2+} in $LiCoO_2$ and Mn^{4+} to Mn^{3+} in $LiMn_2O_4$, while they deintercalate protons on the reverse oxidation. Scanning electron microscopy reveals spherical $LiCoO_2$ particles with a very narrow size distribution. Energy dispersive X-ray detection proved the absence of metal cation intercalation.

Key words Lithium cobaltate · Lithium manganate · Voltammetry · Immobilized microparticles · Proton insertion electrochemistry

Introduction

The electrochemistry of $LiCoO_2$ and $LiMn_2O_4$ in non-aqueous electrolytes has been widely investigated [1, 2], owing to their very promising electrochemical performance in high energy density lithium-ion batteries, involving the electrochemical intercalation and deintercalation of lithium. The electrochemistry of $LiCoO_2$ and $LiMn_2O_4$ in aqueous electrolyte systems has attracted far less attention. In acidic solutions, $LiCoO_2$ is known to undergo Li^+/H^+ exchange reactions [3]. When treated hydrothermally at 200 °C in HCl solutions, it undergoes a proton exchange reaction yielding the iso-structural oxyhydroxide $HCoO_2$. At room temperature, acid acts toward $LiCoO_2$ not only as a delithiating agent but also as a hydrolyzing agent, leading to the formation of metastable $Li_{1-x-y}H_yCoO_2$ [4]. Also, $HCoO_2$ is used as an effective anode material for the oxidation of hydrogen in a solid oxide fuel cell [5]. With regard to lithium manganate, there is an earlier report [6] on electrochemical studies in aqueous electrolyte systems. In 9 M KOH solutions, a pressed electrode of $LiMn_2O_4$ and graphite has been subjected to cyclic voltammetric and charge-discharge studies. Though the proton insertion reaction in $LiMn_2O_4$ from alkali electrolytes has not been proved experimentally, this fact was established and confirmed for γ-MnO_2 in alkali electrolytes, as the material has been intensively investigated for its application in Zn/MnO_2 alkaline batteries. Lithium intercalation in $LiMn_2O_4$ from aqueous LiOH electrolytes has been reported [7].

Recently, in our work on solid $LiNiO_2$ mechanically immobilized on the surface of paraffin-impregnated graphite electrodes, in aqueous alkali electrolytes, we reported proton intercalation and deintercalation accompanied by a Ni^{2+} to Ni^{3+} redox transition [8]. The reduction product of the reaction is assigned to be $LiHNiO_2$, which is similar to the hydrolyzed product $LiHCoO_2$ in acid solutions.

In the present work, we report the synthesis of $LiCoO_2$ and $LiMn_2O_4$ by self-propagating high temperature combustion (SPHTC). This is a novel technique that has been used successfully for the preparation of ceramic and phosphor materials [9–11]. The main advantage of this method, compared to the solid state sintering method, is that the experiment is completed within 10 min. The basic principle of the method is the decomposition of an oxidizer, e.g., a metal nitrate, in the presence of a fuel.

M. Mohan Rao · M. Jayalakshmi · O. Schäf
H. Wulff · F. Scholz (✉)
Institut für Chemie und Biochemie,
Ernst-Moritz-Arndt-Universität Greifswald,
Soldmannstrasse 23, 17489 Greifswald, Germany
e-mail: fschoz@rz.uni-greifswald.de
Tel.: +49-3834-86 4450; Fax: +49-3834-864451

U. Guth
Kurt-Schwabe-Institut für Mess- und Sensortechnik e.V.,
Meinsberg, Germany

The fuel becomes ignited by the oxidizer to yield oxide materials derived from the metal salts.

$LiCoO_2$ and $LiMn_2O_4$ prepared by SPHTC were subjected to electrochemical studies by mechanically immobilizing the solid sample on the surface of a paraffin-impregnated graphite electrode and using aqueous electrolyte systems [12]. We aimed to study the electrochemical behaviour of $LiCoO_2$ and $LiMn_2O_4$ in alkali solutions in order to understand the intercalation and deintercalation of cations during the redox process so that the possible application of these oxides as battery electrode materials in aqueous electrolytes could be examined. With the help of scanning electron microscopy (in conjunction with an energy-dispersive X-ray spectrometer), the electrochemically treated electrodes were analyzed for the presence of intercalated cations. All experimental results can be explained by proton insertion electrochemistry. After finishing this experimental work a publication appeared which confirms proton insertion for sol-gel synthesized $LiMn_2O_4$ [13].

Experimental

Preparation of $LiCoO_2$ and $LiMn_2O_4$ by SPHTC

The $LiCoO_2$ and $LiMn_2O_4$ compounds were prepared according to the procedure reported by our group [8]. The stoichiometry of the reaction mixture was calculated for synthesis of $LiCoO_2$ and $LiMn_2O_4$ as

$$LiNO_3 + Co(NO_3)_2 + 2.5NH_2 - CO - NH_2$$

$$LiNO_3 + 2Mn(NO_3)_2 + 4.2NH_2 - CO - NH_2$$

The required amounts of metal nitrates and urea were dissolved in a minimum amount of distilled water in a quartz beaker. The beaker and solution were subjected to heating in a muffle furnace at 500 °C. After a few minutes the solution boiled, then underwent rapid dehydration followed by decomposition with an intense flame to yield a black fine powder.

Equipment and measurements

For electrochemical measurements the following instrumentation was used: an Autolab (ECO Chemie, Utrecht, Netherlands), an electrode stand VA 663 (Metrohm, Herisau, Switzerland) and a personal computer. The reference electrode (Metrohm, Switzerland) was an Ag/AgCl electrode with 3 M KCl ($E = 0.208$ V vs. SHE). All measurements were performed in solutions which were thoroughly deareated with high-purity nitrogen for at least 10 min. The voltammograms were recorded at 22 ± 1 °C. X-ray diffraction (XRD) measurements were performed with a HZG 4 (Seifert SPM, Germany) and the scanning electron microscope was a Leo 440 (Germany) equipped with an Econ 4 detector (EDAX, USA). All the chemicals used were of analytical grade and all solutions were prepared with double distilled water.

Results and discussion

XRD studies

The XRD patterns of the $LiCoO_2$ and $LiMn_2O_4$ samples prepared by SPHTC are shown in Fig. 1. The patterns

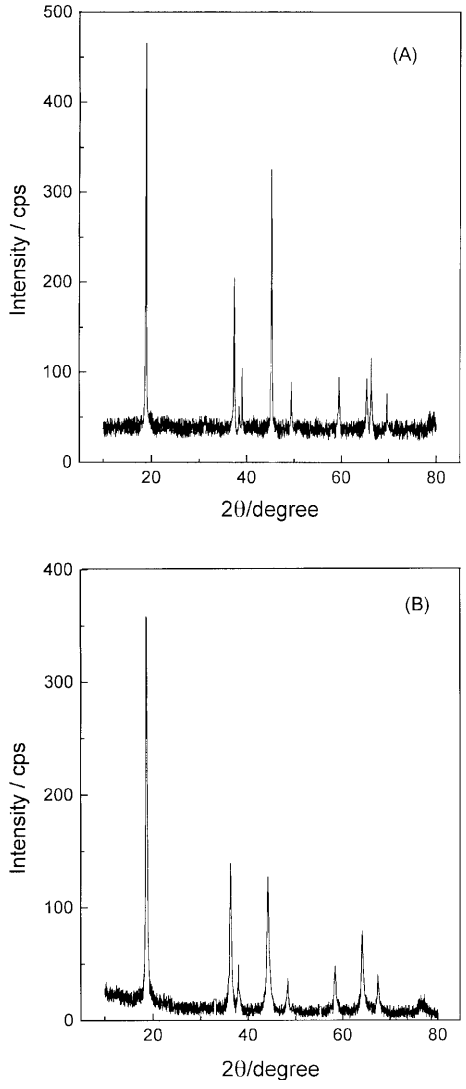

Fig. 1 X-ray diffraction pattern of **A** $LiCoO_2$ and **B** $LiMn_2O_4$

are comparable with the standard JCPDS data and show the formation of single-phase compounds. It has been reported in the literature that $Li_{1-x}CoO_2$ with $0 \le x \le 0.5$ has a layered structure where lithium and cobalt ions fill alternate layers of octahedral sites in a cubic close-packed lattice of oxygen ions. To obtain the exact stoichiometry of the $LiCoO_2$ prepared by SPHTC, the sample was analyzed by inductively coupled plasma (ICP) spectroscopy. The analysis gives the composition of sample prepared by our method as $Li_{0.95}CoO_2$. Unlike $LiCoO_2$, $LiMn_2O_4$ belongs to the spinel system with cubic symmetry (*Fd*3*m*). From ICP analysis the composition of the oxide material was found to be $Li_{0.92}Mn_2O_4$. Scanning electron microscopy (SEM) photographs of $LiCoO_2$ and $LiMn_2O_4$ are shown in Fig. 2. In the case of $LiCoO_2$, the SPHTC produces particles of uniform size (1–3 μm) with a spherical shape. In contrast, the $LiMn_2O_4$ particles are not of uniform size.

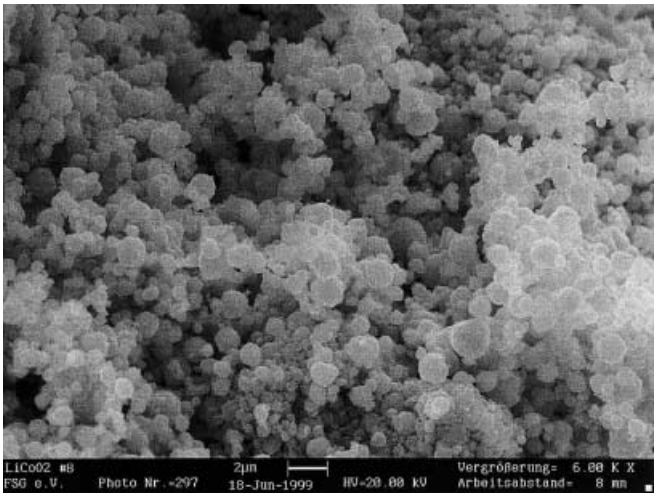

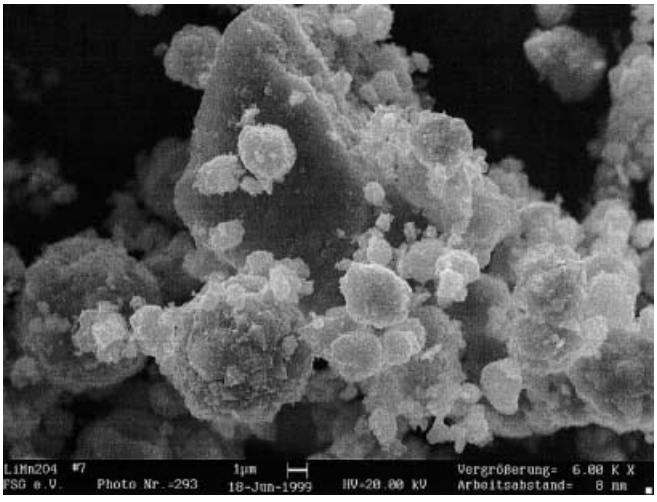

Fig. 2a,b Particle morphology by SEM of samples prepared by SPHTC: **a** $LiCoO_2$; **b** $LiMn_2O_4$

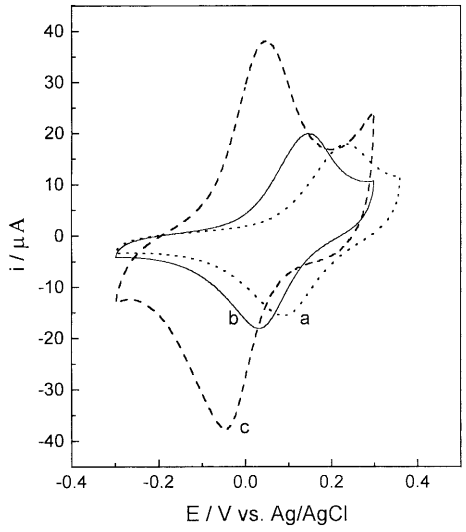

Fig. 3 Cyclic voltammograms of mechanically immobilized $LiCoO_2$ on the surface of a PIGE in different concentrations of KOH electrolyte solutions. Scan rate = 50 mV s^{-1}: *a* 0.05 M; *b* 0.1 M; *c* 1.0 M

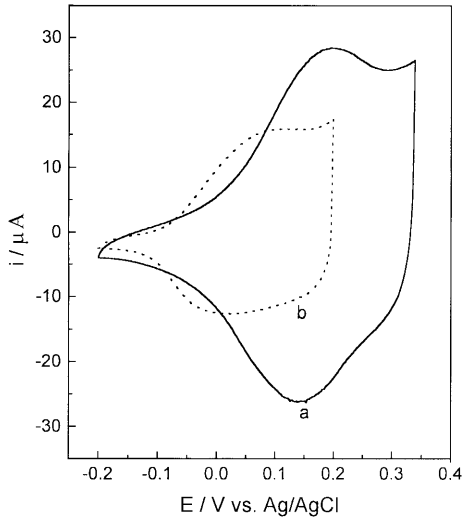

Fig. 4 Cyclic voltammograms of mechanically immobilized $LiCoO_2$ on the surface of a PIGE in different concentrations of LiOH electrolyte solutions. Scan rate = 50 mV s^{-1}: *a* 0.05 M; *b* 0.6 M

Electrochemical studies

Lithium cobaltate

Solid $LiCoO_2$ was mechanically immobilized on the surface of a paraffin-impregnated graphite electrode (PIGE) and cycled in KOH and LiOH solutions. Figures 3 and 4 show the cyclic voltammograms obtained for $LiCoO_2$ in different concentrations of KOH and LiOH solutions, respectively. The cyclic voltammograms reveal a single set of sharp and well-defined redox peaks in the case of KOH solutions, while the peaks are broad and poorly defined in the case of LiOH solutions. The appearance of single set of redox peaks can be explained based on the redox activity of cobalt species in $LiCoO_2$, as it is known that the primary electron donating or accepting centre is cobalt. Hence the anodic peak appeared probably due to the oxidation of Co^{2+} to Co^{3+} in $LiCoO_2$ accompanied by the expulsion of a cation and the cathodic peak may be due to the reduction of Co^{3+} to Co^{2+} accompanied by the intercalation of a cation. The reaction may be written as

$$LiCoO_2 + M^+ + e^- \rightarrow LiMCoO_2$$

Comparing the formal potentials of the redox reaction of $LiCoO_2$ in KOH and LiOH at the same concentration of 0.05 M, it is observed that the formal potential in LiOH (0.18 V) is more positive than the formal potential in KOH (0.12 V). Also, the peak currents increase with increase in KOH concentration, while they decrease with increase in LiOH concentration in the alkali electrolytes. The reason for this difference in electrochemical behaviour of $LiCoO_2$ in KOH and LiOH solutions is not clear, though the variation of activity coefficients in both alkali hydroxide solutions may play a role.

Lithium manganate

When lithium manganate powder was immobilized on a PIGE electrode and cycled in KOH and LiOH solutions, the cyclic voltammetric response was similar to that of lithium cobaltate except for the shift in peak potentials. Figures 5 and 6 show the cyclic voltammograms obtained for $LiMn_2O_4$ in KOH and LiOH solutions, respectively. The cyclic voltammograms exhibit a single set of fairly defined redox peaks in both the solutions. The cathodic peak tends to disappear or appear as a hump in stronger LiOH solutions, as in the case of KOH solutions. It is interesting to note that the change in peak currents with concentration for $LiMn_2O_4$ is contrary to that for $LiCoO_2$. With an increase in KOH concentration the peak currents decrease, while for LiOH the peak currents increase.

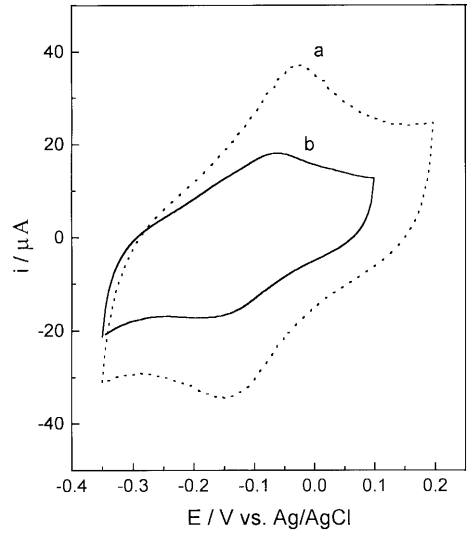

Fig. 5 Cyclic voltammograms of mechanically immobilized $LiMn_2O_4$ on the surface of a PIGE in different concentrations of KOH electrolyte solutions. Scan rate = 50 mV s^{-1}: *a* 0.05 M; *b* 0.1 M

The appearance of single set of redox peaks for $LiMn_2O_4$ in alkali electrolyte solutions has to be associated with the oxidation or reduction of manganate species accompanied by expulsion or insertion of a cation, most probably a proton. The redox reaction may be written as

$$LiMn_2O_4 + M^+ + e^- \rightarrow LiMMn_2O_4$$

where the identity of the cation intercalated from aqueous electrolytes has to be examined and confirmed.

In the present work, we observed only one set of peaks for $LiMn_2O_4$ in both KOH and LiOH solutions at all scans. There is no dramatic change in cyclic voltammetric behaviour from initial to successive scans as observed in the case of pressed $LiMn_2O_4$ [6] in 9 M KOH solutions (0.5 mV s^{-1}), where the reason for this disparity has been attributed to structural changes and poor rechargeability. In the non-aqueous electrochemistry of lithium manganate, it has been shown that the amount of lithium inserted and the reversibility of lithium insertion/extraction reactions depend strongly on the route by which the compound is prepared [14] since the structure, morphology and composition are concurrently affected by the preparation procedure.

In order to compare the electrochemical behaviour of γ-MnO_2 with that of $LiMn_2O_4$ under similar experimental conditions, γ-MnO_2 was mechanically immobilized on the surface of a PIGE and cycled in KOH solutions. Figure 7 shows the cyclic voltammogram obtained in 0.1 M KOH solution at the scan rate of 0.05 V s^{-1}. As in $LiMn_2O_4$, there is a single set of redox peaks but there is a definite difference in peak potentials. The CV response is a stabilized one after 10 cycles and there

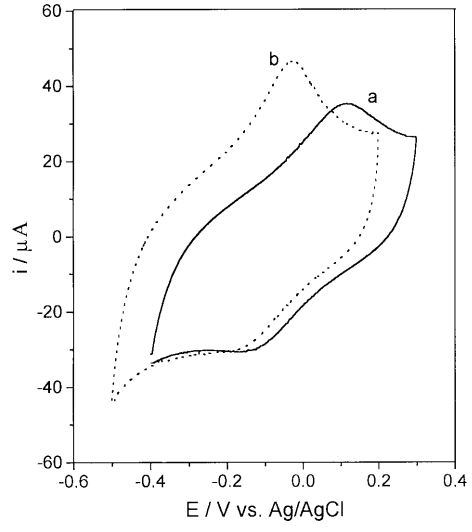

Fig. 6 Cyclic voltammograms of mechanically immobilized $LiMn_2O_4$ on the surface of a PIGE in different concentrations of LiOH electrolyte solutions. Scan rate = 50 mV s^{-1}: *a* 0.01 M; *b* 0.1 M

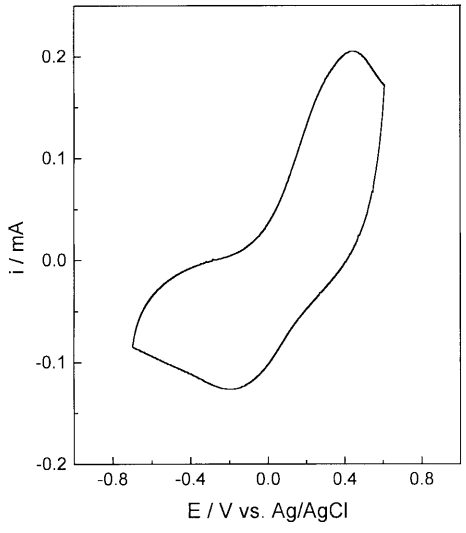

Fig. 7 Cyclic voltammogram of mechanically immobilized γ-MnO_2 on the surface of a PIGE in 0.1 M KOH electrolyte solution at the scan rate of 50 mV s^{-1}

is no decrease of peak currents with cycling. In this potential region the peaks appear due to the homogeneous solid-state reduction of γ-MnO_2 to MnOOH and reoxidation, which is controlled by the simultaneous uptake of electrons and protons [15]. This CV behaviour is contradictory to earlier reports, where a complex spectrum with multiple peaks is observed for either pressed γ-MnO_2 [6] or mechanically abrased γ-MnO_2 [16, 17] in 9 M KOH solutions. In the present case, the absence of multiple peaks may be due to either the high scan rates employed or the low alkali concentrations used. Also, the redox reaction is more reversible in $LiMn_2O_4$ than in γ-MnO_2.

Identity of cation

As mentioned in the introductory part of this paper, $LiCoO_2$ undergoes proton exchange reactions in acid solutions. At room temperature, $LiCoO_2$ forms $LiHCoO_2$, a resultant product of reduction, delithiation and hydrolysis [4], but for $LiMn_2O_4$ the resulting material after lithium extraction by acid treatment was reported to be λ-MnO_2 [18]. It is necessary to point out that these are solution phase reactions. It has been reported [19] that the oxidation-reduction capability of insertion materials is the same as those of redox systems in solution, though the situation is quite different from conventional redox systems. It is difficult to assign an exact valence state for each species and to separate the effect of cations from that of electrons upon the redox potentials. Unlike in solution phase reactions, in this case the redox potentials are established based on the transfer of cations across the solid/liquid interface, which is characteristic of an insertion reaction. In the present study, solid $LiCoO_2$ or $LiMn_2O_4$ was mechanically immobilized on the surface of a PIGE and cycled in alkali electrolyte solutions, and the history of formal potentials derived from the redox peak potentials of cyclic voltammograms would reflect the identity of the cation intercalated in the above-mentioned redox transformations.

If we suppose that the intercalating cation is an alkali metal cation (K^+ or Li^+) in these alkali electrolytes, then the equation representing the redox reaction may be written as

$$LiCoO_2 + K^+ + e^- \rightarrow LiKCoO_2$$

In accordance with this reaction one should, according to Nernst, observe the following dependence of the formal potential on activity of the alkali cation:

$$E_f = E^\circ + 0.059 \log a_{K^+}$$

i.e. the formal potential $E_f = (E_a + E_c)/2$ of the redox reaction should be directly proportional to the logarithm of potassium ion activity in KOH electrolyte solutions. Table 1 shows the formal potentials evaluated in various concentrations of KOH electrolyte. As seen from the table, the formal potentials decrease with an increase in concentration of the alkali electrolyte solutions. This fact is more clear from the derived plot of E_f vs. $\log[K^+]$ in Fig. 8. These results indicate that the alkali metal cations do not intercalate in $LiCoO_2$ from alkali electrolyte solutions. If we assume that the intercalating cation is a proton, then the equation for the redox reaction can be written as

$$H^+ + LiCoO_2 + e^- \rightarrow LiHCoO_2$$

Then, the Nernst equation follows as:

$$E_f = E^\circ + 0.059 \log a_{H^+}$$

In this case, the formal potentials should be directly proportional to the logarithm of the proton activity in the alkali electrolyte solutions. The negative slope of the plot in Fig. 8 is in good agreement with the idea of proton participation in the redox reaction.

The same argument holds good for $LiMn_2O_4$ also. Table 2 presents the formal potentials evaluated in various concentrations of KOH electrolytes. With an increase in the concentration of the alkali electrolyte solutions, the formal potentials decrease in both cases. The proton intercalation in $LiMn_2O_4$ is further clarified by the derived plots of E_f vs. $\log[K^+]$ in Fig. 8. The negative slope of the plot confirms the idea of the participation of protons in the redox reaction. SEM-energy dispersive X-ray (EDX) results carried out in electrochemically treated $LiMn_2O_4$ support this supposition, which will be discussed in forthcoming paragraphs.

Table 1 Formal potentials of the $Co^{2+/3+}$ system for solid $LiCoO_2$ at various concentrations of KOH electrolyte solutions

Conc. KOH (mol dm^{-3})	0.05	0.1	0.3	0.6	1.0
E_f (mV) vs. Ag/AgCl	118	89	52	25.5	0.02

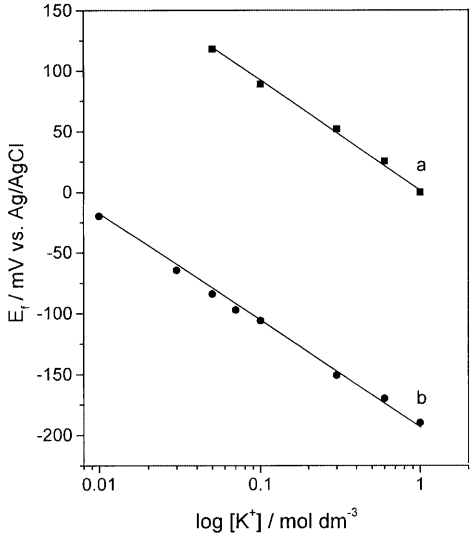

Fig. 8 Derived plots of E_f vs. $\log[K^+]$ for *a* $LiCoO_2$ and *b* $LiMn_2O_4$

Table 2 Formal potentials of the $Mn^{3+/4+}$ system for solid $LiMn_2O_4$ at various concentrations of KOH electrolyte solutions

Conc. KOH (mol dm^{-3})	0.01	0.03	0.05	0.07	0.1	0.3	0.6	1.0
E_f (mV) vs. Ag/AgCl	−19.8	−64.5	−84	−97.1	−106	−150.8	−170	−190

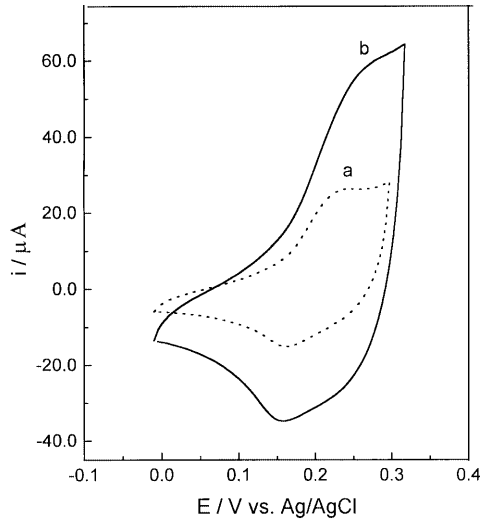

Fig. 9 Cyclic voltammograms of mechanically immobilized $Co(OH)_2$ on the surface of a PIGE in 0.1 M KOH electrolyte solution. Scan rate: *a* 10 mV s^{-1}; *b* 50 mV s^{-1}

$Co(OH)_2$/CoOOH conversion

$LiCoO_2$ forms $LiHCoO_2$ by reduction and proton uptake, which is reported to be similar and iso-structural to the oxyhydroxide of Co. In order to understand this reaction product obtained by electrochemical reversible proton intercalation in our studies, cyclic voltammograms were recorded for $Co(OH)_2$/CoOOH conversion and compared with that of $LiCoO_2$. Cobalt hydroxide was prepared by chemical precipitation of cobalt nitrate and excess KOH solutions The precipitate was washed and dried at 100 °C. XRD confirmed the formation of $Co(OH)_2$ This powder was mechanically immobilized on the surface of a PIGE and cycled in 0.1 M KOH solution. The cyclic voltammograms with a single set of redox peaks at scan rates of 0.01 and 0.05 V s^{-1} are shown in Fig. 9. At the lower scan rate, the anodic peak occurred at 0.24 V and the cathodic peak at 0.16 V, and the formal potential of this redox reaction is 0.2 V. The redox reaction responsible for this set of peaks for $Co(OH)_2$ in KOH solution may be written as

$$Co(OH)_2 \rightarrow CoOOH + H^+ + e^-$$

This reaction is analogous to $Ni(OH)_2$/NiOOH conversion reported in Ni/Cd and Ni/H_2 batteries.

On comparing the cyclic voltammograms obtained for $LiCoO_2$ and $Co(OH)_2$ in 0.1 M KOH solution at the same scan rate of 0.05 V s^{-1}, there were noticeable differences in peak shapes, peak and formal potentials. The formal potential of $LiCoO_2/LiHCoO_2$ was 0.089 V while that of $Co(OH)_2$/CoOOH was 0.2 V. This result lead us to believe that the proton intercalation product of $LiCoO_2$ is not the oxyhydroxide form of Co, though in situ spectral studies are needed to confirm this belief.

SEM-EDX studies

The SEM-EDX spectra obtained for $LiCoO_2$ and $LiMn_2O_4$ powders prior to electrochemical treatment show only Co and Mn signals. As expected, there was no intercalated cation in the sample. Also the EDX spectra of $LiCoO_2$ and $LiMn_2O_4$ samples which were electrochemically treated did not show any other metal than cobalt and manganese, respectively. The samples were subjected to a cycle of intercalation/deintercalation processes through chronocoulometric and cyclic voltammetric experiments. The absence of a signal for K^+ ions in the EDX spectrum reveals that these ions do not intercalate during the redox reaction. These results clearly augment our arguments and conclusions arrived through electrochemical studies.

Acknowledgements M.J. acknowledges provision of a fellowship from Humboldt Stiftung (AvH) and M.M.R. acknowledges a postdoctoral fellowship from Deutsche Forschungsgemeinschaft (DFG). The authors thank Mrs. Inge Fabian (Humboldt-Universität zu Berlin) for performing the ICP analyses and Fonds der Chemischen Industrie for support.

References

1. Rahner D, Machill S, Schlörb H, Siury K, Kloss M, Plieth W (1998) J Solid State Electrochem 2: 78
2. Alcantara R, Lavela P, Tirado JL, Zhecheva E, Stojanova R (1999) J Solid State Electrochem 3: 121
3. Fernandez JM, Hernan L, Morales J, Tirado JL (1988) Mater Res Bull 23: 899
4. Zhecheva E, Stojanova R (1994) J Solid State Chem 109: 47
5. Sato K, Hagizaka S, Inoue Y (1993) Solid State Ionics 66: 197
6. Schlörb H, Bungs M, Plieth W (1997) Electrochim Acta 42: 2619
7. Li W, Mckinnon WR, Dahn JR (1994) J Electrochem Soc 141: 2310
8. Mohan Rao M, Jayalakshmi M, Schäf O, Wulff H, Guth U, Scholz F (1999) J Solid State Electrochem 4: 17
9. Kottaisamy M, Jayakumar D, Jagannathan R, Mohan Rao M (1996) Mater Res Bull 31: 1013
10. Kottaisamy M, Mohan Rao M, Jayakumar D (1997) J Mater Chem 7: 345
11. Manoharan SS, Patil KC (1992) J Am Ceram Soc 75: 1012
12. Scholz F, Meyer B (1998) Voltammetry of solid microparticles immobilized on electrode surfaces. In: Bard AJ, Rubinstein I (eds) Electroanalytical chemistry, a series of advances, vol 20. Dekker, New York, pp 1–86

13. Cachet-Vivier C, Bach S, Pereira-Ramos JP (1999) Electrochim Acta 44: 2705
14. Barboux P, Tarascon JM, Shokoohi FK (1991) J Solid State Chem 94: 185
15. Kozawa A (1974) Manganese dioxide. In: Kordesch KV (ed) Batteries, vol 1. Dekker, New York, p 385
16. Fiedler DA, Besenhard JO, Fooken MH (1997) J Power Sources 69: 11
17. Fiedler DA (1998) J Solid State Electrochem 2: 315
18. Hunter JC (1981) J Solid State Chem 39: 142
19. Ohzuku T, Ueda A (1994) Solid State Ionics 69: 201